

Robust cell-free mmWave/sub-THz access using minimal coordination and coarse synchronization

Lorenzo Miretti Member, IEEE, Giuseppe Caire Fellow, IEEE, Sławomir Stańczak Senior Member, IEEE

Abstract—This study investigates simpler alternatives to coherent joint transmission for supporting robust connectivity against signal blockage in mmWave/sub-THz access networks. By taking an information-theoretic viewpoint, we demonstrate analytically that with a careful design, full macrodiversity gains and significant SNR gains can be achieved through canonical receivers and minimal coordination and synchronization requirements at the infrastructure side. Our proposed scheme extends non-coherent joint transmission by employing a special form of diversity to counteract artificially induced deep fades that would otherwise make this technique often compare unfavorably against standard transmitter selection schemes. Additionally, the inclusion of an Alamouti-like space-time coding layer is shown to recover a significant fraction of the optimal performance. Our conclusions are based on an insightful multi-point intermittent block fading channel model that enables rigorous ergodic and outage rate analysis, while also considering timing offsets due to imperfect delay compensation. Although simplified, our approach captures the essential features of modern mmWave/sub-THz communications, thereby providing practical design guidelines for realistic systems.

Index Terms—mmWave, sub-THz, cell-free, non-coherent joint transmission, space-time coding, macrodiversity, synchronization.

I. Introduction

A well-known major problem in mobile access networks operating at very high carrier frequencies, such as in the upper mmWave or sub-THz bands, is that they are highly sensitive to signal blockage [?], [?], [?]. The reason is due to unavoidable physical characteristics of the propagation medium as well as the expected mode of operation, which relies on highly directional line-of-sight transmission in the noise limited regime [?], [?], [?]. This sensitivity causes connection instability and severely degrades the overall system performance.

In order to mitigate the signal blockage and provide robust connectivity, several multi-connectivity concepts are advocated by academia, industry, and standardization bodies [?], [?], [?], [?]. In fact, a similar trend is also followed in the context of visible light communication [?], where signal blockage is an evident issue. Essentially, all these concepts attempt to capitalize on the so-called macrodiversity gains offered by simultaneous and possibly

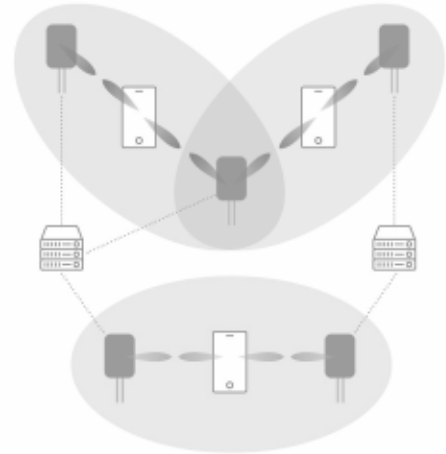


Fig. 1. Network of multiple transmitters simultaneously connected to multiple receivers via high-rate and directional mmWave/sub-THz links. Compared to conventional mmWave/sub-THz cellular networks, this architecture has a great potential to offer robust connectivity against signal blockages. The key aspect covered in this study is how to realize this and possibly other benefits using low complexity and cost-effective devices and network infrastructure.

coordinated connections to multiple access points. The proposed technologies range from relatively simple control plane approaches for fast and efficient access point selection [?], [?], [?], to data plane approaches that involve, for instance, concurrent transmission over orthogonal resources (i.e., parallel channels) [?], or even advanced network multiple-input multiple-output (MIMO) techniques based on joint processing of distributed antenna systems [?], [?], [?]. The present study considers variations of the latter technology, focusing on downlink transmission.

A. Summary of prior studies

The use of network MIMO techniques in distributed antenna systems has gained significant attention due to its potential to provide the best theoretical performance among all multi-connectivity concepts [?]. However, the classical literature on network MIMO is typically based on ideal assumptions and often does not cover the specific characteristics of mmWave/sub-THz network MIMO systems, in particular in terms of channel models, hardware capabilities, and energy efficiency aspects. Therefore, it may lead to misleading conclusions for practical implementations. These limitations are addressed by several recent studies, focusing on different aspects of mmWave/sub-THz network MIMO systems. For example, [?] studies

L. Miretti, G. Caire, and S. Stańczak are with the Technische Universität Berlin, Berlin 10587, Germany (email: {miretti, caire, stanczak}@tu-berlin.de). L. Miretti and S. Stańczak are also with the Fraunhofer Institute for Telecommunications Heinrich-Hertz-Institut HHI, Berlin 10587, Germany.

realization, the ergodic capacity can be then approached by means of rate adaptation mechanisms based on CSIT α . Note that an intermediate solution in terms of latency is to use hybrid automatic retransmission-request (H-ARQ) mechanisms [?], which also require some form of CSIT.

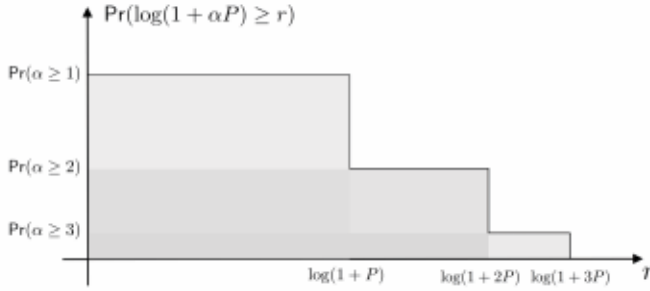


Fig. 2. Pictorial representation of the CCDF of the instantaneous capacity.

As a more appropriate performance metric in the presence of strict latency constraints and when rate adaptation mechanisms based on CSIT are prohibitive, we now study the outage capacity of the considered channel. In particular, by considering fixed-rate block codes of maximum length T , we measure capacity as

$$C_{\text{out}} := \sup_{r \in \mathbb{R}} r \cdot \Pr(\log(1 + \alpha P) \geq r).$$

Proposition 2. The outage capacity of the considered channel with power constraint $P \in \mathbb{R}_+$ per transmitter is given by

$$C_{\text{out}} = \max_{i \in \{1, \dots, L\}} \Pr(\alpha \geq i) \log(1 + iP). \quad (3)$$

Proof. The proof readily follows by observing that $\Pr(\log(1 + \alpha P) \geq r)$ is a decreasing step function of r with discontinuities located at $\log(1 + iP)$ and step heights $\Pr(\alpha \geq i)$, for $i \in \{1, \dots, L\}$. \square

The quantitative difference between the ergodic and outage capacity can be visualized in Figure ??, which depicts the complementary cumulative density function (CCDF) of the instantaneous capacity $\log(1 + \alpha P)$. The ergodic capacity is given by the total area underlying the CCDF, while the outage capacity is given by the largest rectangle. The two metrics are also compared in terms of different parameters in Figure ??.

III. Practical transmission schemes

In this section we revisit, compare, and extend a set of practical transmission schemes that do not require the receiver to perform complex decoding algorithms. We will measure performance in terms of ergodic and outage rates, depending on the context and applicability, and discuss crucial implementation aspects.

A. Transmitter selection

As first main baseline, we consider a transmission scheme where, for each t th block-fading realization with at least one non-blocked transmitters, i.e., such that $\alpha_t > 0$,

the network chooses one non-blocked transmitter $l^*(\beta_t)$ and lets $(\forall m \in \mathbb{Z}) (\forall l \in \{1, \dots, L\})$

$$x_l[m] = \begin{cases} u[m] & \text{if } l = l^*(\beta_t) \text{ and } \alpha_t > 0, \\ 0 & \text{otherwise,} \end{cases} \quad t = \left\lfloor \frac{m}{T} \right\rfloor,$$

where $u[m] \sim \mathcal{CN}(0, P)$ is a scalar i.i.d. information bearing signal. By mapping this scheme to some $\mathbf{Q} \in \mathcal{Q}$ in the signal model (??), it can be readily seen that the ergodic rate

$$R = (1 - p_B^L) \log(1 + P)$$

is achievable. Note that the concept of outage rate is not meaningful for this scheme, since the outage events are known by the network. The main advantage of transmitter selection is that it can mitigate the effect of blockage using simple scalar codes at fixed rate $\log(1 + P)$. However, this simplicity comes with two major drawbacks. First, no SNR gain is provided, i.e., R saturates to $\log(1 + P)$ as L grows. Second, causal knowledge of β_t at the transmitters is assumed. Alternatively, the choice of the transmitter can be performed by the receiver, but this procedure still entails the timely feedback of $l^*(\beta_t)$ to the network. Overall, the required resources for timely blockage estimation and network coordination may be significant, especially in case of frequent blockages.

B. Non-coherent joint transmission

As second main baseline, we consider non-coherent joint transmission of a single scalar codeword from all transmitters simultaneously, i.e., we let $(\forall m \in \mathbb{Z}) (\forall l \in \{1, \dots, L\})$

$$x_l[m] = u[m],$$

where $u[m] \sim \mathcal{CN}(0, P)$ is a scalar i.i.d. information bearing signal. Using (??), we observe that this scheme achieves the ergodic rate

$$R = \mathbb{E}[\log(1 + |h|^2 P)], \quad (4)$$

where $h := \sum_{l=1}^L \beta_l e^{j\theta_l}$ denotes an effective small-scale fading coefficient which is artificially induced by the non-coherent superposition of signals at the receiver.

Non-coherent joint transmission always outperforms transmitter selection in terms of ergodic rates, and it provides SNR gains as L grows. This trend is clearly visible in Figure ?. For a formal proof, we exploit the following intuitive property, which essentially states that, on average, adding non-blocked transmitters is beneficial.

Proposition 3. Let $\{\theta_l\}_{l=1}^\infty$ be an i.i.d. random process with first order distribution $\text{Uniform}(0, 2\pi)$. Then, the sequence $\{\bar{R}(i)\}_{i=0}^\infty$ given by $(\forall i \geq 0)$

$$\bar{R}(i) := \mathbb{E} \left[\log \left(1 + \left| \sum_{l=1}^i e^{j\theta_l} \right|^2 P \right) \right] \quad (5)$$

is strictly increasing and unbounded above, i.e.,

$$(\forall i \geq 0) \bar{R}(i+1) > \bar{R}(i), \text{ and } \lim_{i \rightarrow \infty} \bar{R}(i) = \infty.$$

Proof. The proof is given in Appendix ?. \square

The gains of non-coherent joint transmission can be then formalized as follows.

Proposition 4. The ergodic rate in (??) achieved by non-coherent joint transmission satisfies:

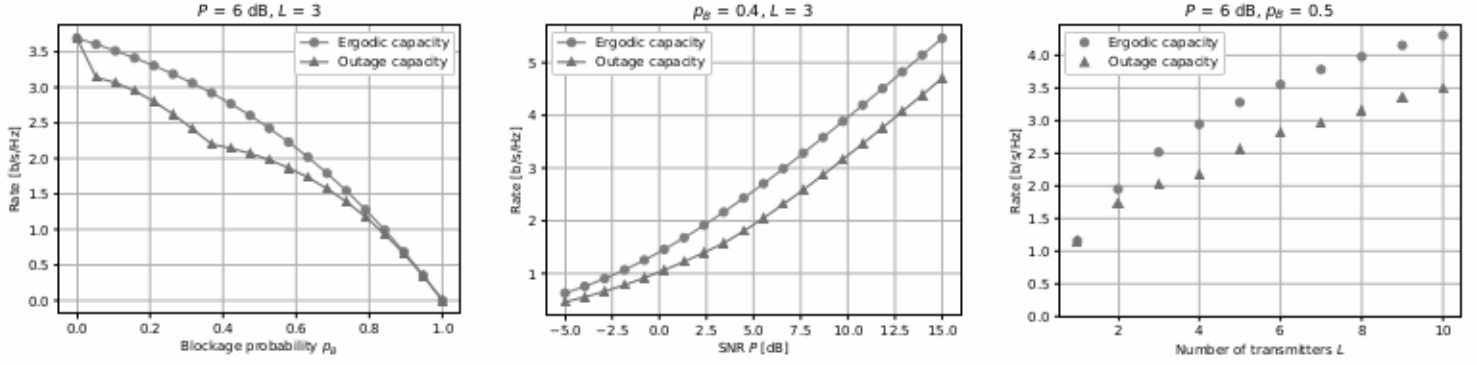


Fig. 3. Ergodic and outage capacity versus blockage probability, SNR, and number of transmitters.

- (i) $(\forall L \geq 1) R \geq (1 - p_B^L) \log(1 + P)$;
- (ii) R is a strictly increasing sequence in L ;
- (iii) $\lim_{L \rightarrow \infty} R = \infty$.

Proof. The proof is given in Appendix ??.

However, these potential gains may be very difficult to achieve in practice. In fact, although no CSIT is theoretically needed, practical coding schemes based on rate adaptation or HARQ mechanisms need to track and adapt to the instantaneous rate fluctuations $\log(1 + |h|^2 P)$. Unfortunately, the instantaneous rate $\log(1 + |h|^2 P)$ fluctuates at a much faster pace and over a much larger dynamic range than for the case of transmitter selection, where the fluctuations are driven by the blockage process only. Therefore, it is not clear whether non-coherent joint transmission is indeed preferable over transmitter selection when the resources consumed by these mechanisms must be taken into account.

To study the performance of a more practical non-adaptive low-latency implementation of non-coherent joint transmission, we consider the outage rate

$$R_{\text{out}} = \sup_{r \in \mathbb{R}} r \cdot \Pr(\log(1 + |h|^2 P) \geq r).$$

The main advantage of this implementation is that it requires minimal coordination effort at the network side. However, our numerical results show that the outages due to the artificially induced small-scale fading can be significant, and that there are non-trivial dependencies on the system parameters. In particular, by comparing Figure ?? and Figure ??, we can see that R_{out} is well below $(1 - p_B^L) \log(1 + P)$ (i.e., the performance of transmitter selection) in most cases of interest. Hence, the simplicity of non-coherent joint transmission may come at a significant price in terms of performance, which is satisfactory for very specific cases only, such as the case of a very large number of transmitters.

C. Phase diversity

To address the limitations of non-coherent joint transmission, in this section we propose an extension (based on so-called phase diversity [??]) that mitigates the detrimental impact of the artificially induced small-scale fading. The main idea is to induce a controlled fast-fading regime

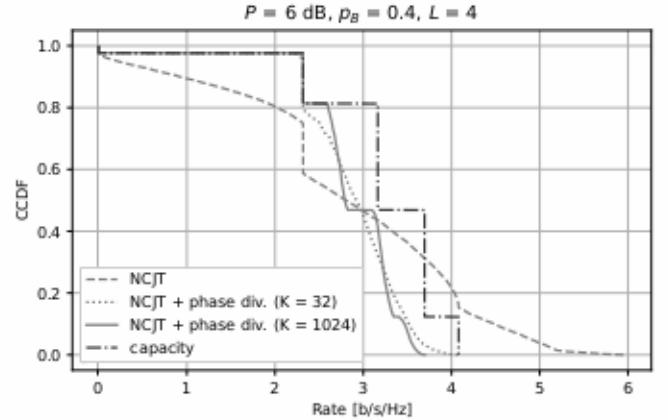


Fig. 4. CCDF of the instantaneous capacity, and of the instantaneous rate of non-coherent joint transmission (NCJT) with and without phase diversity.

for escaping deep fading bursts. We split each fading block of length T into an integer number $M = T/K$ of frames composed by K symbols each. For convenience, we rearrange the time-domain channel model onto a grid model (similar to an OFDM grid) as follows: $(\forall m \in \mathbb{Z})$ $(\forall k \in \{1, \dots, K\})$

$$y[m, k] = \sum_{l=1}^L h_{l,t} x_l[m, k] + z[m, k], \quad t = \left\lfloor \frac{m}{M} \right\rfloor. \quad (6)$$

We then let $(\forall m \in \mathbb{Z})$ $(\forall k \in \{1, \dots, K\})$ $(\forall l \in \{1, \dots, L\})$

$$x_l[m, k] = e^{j\phi_{l,k}} u[m, k], \quad (7)$$

where $u[m, k] \sim \mathcal{CN}(0, P)$ is a scalar i.i.d. information bearing signal, and where $(\forall l \in \{1, \dots, L\})$ $(\phi_{l,1}, \dots, \phi_{l,K})$ is a vector of random phases independently and uniformly distributed in $[0, 2\pi]$, which is shared among the transmitters and receiver as a common source of randomness. Provided that the number of frames M is large enough, standard arguments (as the ones used, e.g., for coding in OFDM systems) show that the following outage rate is achievable:

$$R_{\text{out}} = \sup_{r \in \mathbb{R}} r \cdot \Pr\left(\frac{1}{K} \sum_{k=1}^K \log(1 + |h[k]|^2 P) \geq r\right),$$

where $h[k] := \sum_{l=1}^L \beta_l e^{j(\theta_l + \phi_{l,k})}$ denotes an effective small-scale fading coefficient that fluctuates within the same

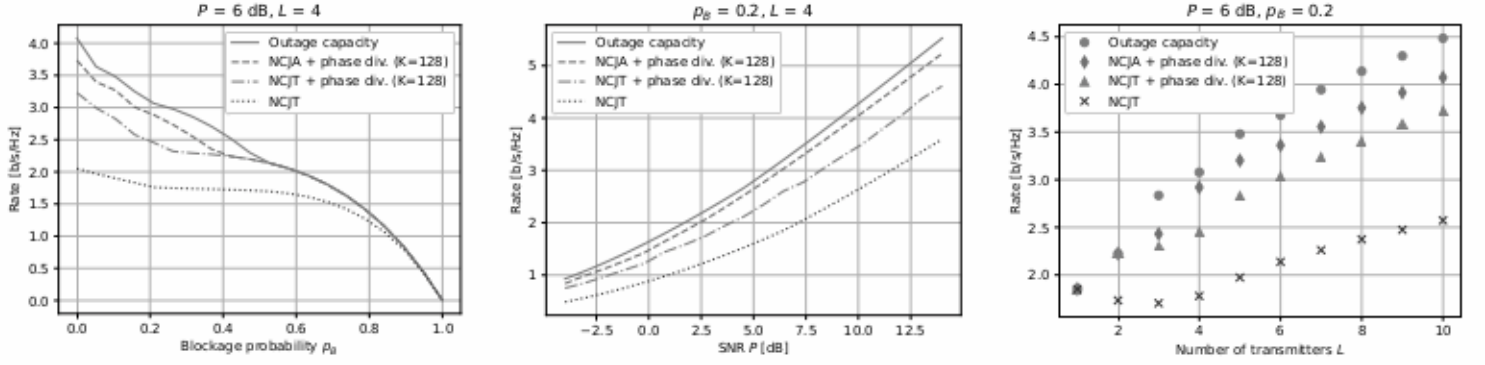


Fig. 5. Outage rate achieved by non-coherent joint transmission (NCJT) without phase diversity, NCJT with phase diversity, non-coherent joint Alamouti space-time coding (NCJA) with phase diversity, and capacity achieving schemes, under different system parameters.

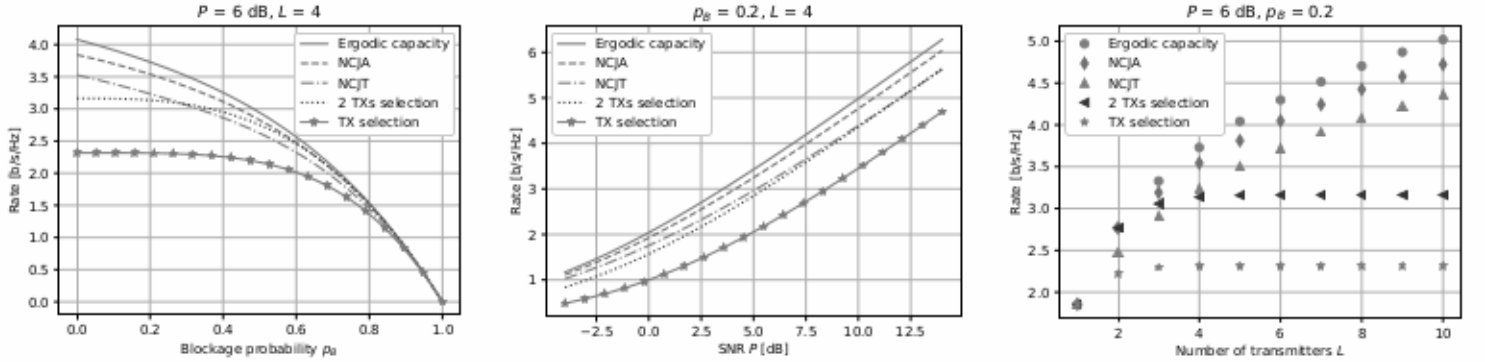


Fig. 6. Ergodic rate achieved by transmitter selection, non-coherent joint transmission (NCJT), two transmitters selection, non-coherent joint Alamouti space-time coding (NCJA), and capacity achieving schemes, under different system parameters. NCJT and NCJA can be with or without phase diversity.

frame of K symbols, according to the given vector of random phases. The proposed extension is motivated by the following asymptotic property:

Proposition 5. For all $i \in \{0, \dots, L\}$, let $\bar{R}(i)$ as in (??). Then, $(\forall \epsilon > 0)$

$$\lim_{K \rightarrow \infty} \Pr \left(\left| \frac{1}{K} \sum_{k=1}^K \log(1 + |h[k]|^2 P) - \bar{R}(\alpha) \right| \geq \epsilon \right) = 0,$$

i.e., the instantaneous rate converges in probability to $\bar{R}(\alpha)$ as K grows large.

Proof. The proof is based on the weak law of large numbers. The details are given in Appendix ??.

The above proposition suggests that the proposed extension of non-coherent joint transmission can reduce the effect of the artificially induced small-scale fading, and make the instantaneous rate fluctuations be essentially driven by the aggregate blockage process α . This effect is clearly visible in Figure ??, where the CCDF of the instantaneous rate approaches $\Pr(\bar{R}(\alpha) \geq r)$, i.e., a step-wise function similar to the CCDF of the instantaneous capacity $\log(1 + \alpha P)$, as K grows. The difference between these two functions is a Jensen's penalty for the disconti-

nities indexed by $i \geq 2$, since $(\forall i \geq 1) \bar{R}(i) \leq \log(1 + iP)$ holds, with equality for $i = 1$.

An important consequence of this behavior is that, in contrast to simple non-coherent joint transmission, the outage rate is (asymptotically) larger or equal than the ergodic rate achieved by transmitter selection. This property can be easily formalized as follows:

Proposition 6. Let $\bar{R}_{\text{out}} = \sup_{r \in \mathbb{R}} r \cdot \Pr(\bar{R}(\alpha) \geq r)$ be the outage rate asymptotically achievable by the proposed extension of non-coherent joint transmission. Then:

$$\bar{R}_{\text{out}} = \max_{i \in \{1, \dots, L\}} \Pr(\alpha \geq i) \bar{R}(i).$$

Proof. Same steps as in the proof of Proposition ??.

Corollary 2. The following inequality holds:

$$\bar{R}_{\text{out}} \geq \Pr(\alpha \geq 1) \bar{R}(1) = (1 - p_B^L) \log(1 + P).$$

Despite the asymptotic nature of the above property, our numerical results in Figure ?? and Figure ?? show that similar conclusions may hold also for moderate values of K . Therefore, at the price of a slight increase in channel coding complexity (comparable to OFDM systems), the proposed extension can achieve the same or better effective rates as transmitter selection, without requiring fast net-

work coordination and rate adaptation mechanisms based on CSIT.

In terms of ergodic rates, the proposed extension achieves

$$R = \mathbb{E} \left[\frac{1}{K} \sum_{k=1}^K \log(1 + |h[k]|^2 P) \right] = \mathbb{E}[\log(1 + |h|^2 P)],$$

that is, it does not provide any performance gain with respect to simple non-coherent joint transmission. However, the proposed extension is still very useful for the ergodic regime, since it significantly reduces the required complexity for approaching the ergodic rate via rate adaptation. Essentially, for large enough K , the encoder needs only to choose one out of L coding rates, based on casual knowledge of the realizations α of the aggregate blockage process, as for the capacity achieving scheme. Similarly, the reduced fluctuations may significantly simplify the design of HARQ schemes.

Remark 1. The proposed extension is based on the so-called phase diversity scheme [?], which can be interpreted as a generalization of other known forms of diversity. In particular, the specific realization $(\forall l \in \{1, \dots, L\})$ $(\forall k \in \{1, \dots, K\})$ $\phi_{l,k} = 2\pi(k-1)d_l/K$ for some $d_l \in \mathbb{N}$ gives the same performance and grid model in (??) as the so-called cyclic delay diversity scheme [?], which is implemented by applying at each l th transmitter a cyclic shift d_l to each frame of K symbols, and by performing frequency-domain processing. This effectively corresponds to introducing frequency diversity, although the original channel is not frequency selective. We remark that this form of diversity have been mostly studied under classical multi-antenna fading models with rich scattering, such as the i.i.d. Rayleigh fading model, for which the effect of small-scale fading cannot be significantly mitigated by means of phase rotations at each antenna, as in this study.

D. Space-time coding

For the special case of $L = 2$ transmitters, the well-known Alamouti space-time block coding scheme [?] achieves both the ergodic and outage capacity by using simple linear receiver processing and scalar decoding, since it converts the original channel model into the effective single-input single-output model $(\forall m \in \mathbb{Z})$

$$y[m] = \sqrt{\alpha_t} u[m] + z[m], \quad t = \left\lfloor \frac{m}{T} \right\rfloor,$$

where $u[m]$ is a scalar information bearing signal, which we assume i.i.d. $\mathcal{CN}(0, P)$. Unfortunately, the remarkable performance and simplicity of the Alamouti scheme cannot be extended to $L > 2$ transmitters [?]. However, space-time coding schemes for $L > 2$ transmitters with reasonable complexity-performance trade-off are still worthy of investigation. One possibility would be to revisit the available studies on some special classes of high-rate low-complexity space-time codes, such as quasi-orthogonal space-time block codes [?], linear dispersion codes [?], or similar alternatives, in light of the intermittent block fading model considered in this study. However, we leave this line of research for future work, and focus on the

following simple enhancements of the transmitter selection and phase diversity schemes by means of an Alamouti space-time coding stage.

1) Two transmitters selection: For each t th block-fading realization with at least one non-blocked transmitters, i.e., such that $\beta_t \neq \mathbf{0}$, the network chooses a pair of transmitters $(l^*, l'^*)(\beta_t)$ such that $(\beta_{l^*,t}, \beta_{l'^*,t}) \neq (0, 0)$, and let them transmit the same scalar information bearing signal using Alamouti space-time coding. The other transmitters remain silent, as in the transmitter selection scheme. Similar to the case of $L = 2$ transmitters, linear receiver processing converts the original channel model into the effective single-input single-output channel model $(\forall m \in \mathbb{Z})$

$$y[m] = \sqrt{\min(2, \alpha_t)} u[m] + z[m], \quad t = \left\lfloor \frac{m}{T} \right\rfloor,$$

where $u[m]$ is a scalar information bearing signal, which we assume i.i.d. $\mathcal{CN}(0, P)$. The following ergodic rate is achievable using standard techniques:

$$R = \Pr(\alpha \geq 2) \log(1 + 2P) + \Pr(\alpha = 1) \log(1 + P).$$

This scheme always outperforms transmitter selection, since it exploits the SNR gain offered by simultaneous transmissions from two transmitters. In contrast, the comparison against a non-coherent joint transmission is non-trivial and highly dependent on the system parameters, as also shown in Figure ??.

2) Non-coherent joint Alamouti space-time coding with phase diversity: We consider the same grid channel model in (??), and cluster the transmitters in pairs. For each pair of transmitters, we modify the transmit signals in (??) by replacing the i.i.d information bearing signal $u[m, k]$ with its Alamouti space-time coded version (spanning two consecutive K -dimensional frames indexed by m). Linear receiver processing leads to the effective single-input single-output channel model $(\forall m \in \mathbb{Z})$ $(\forall k \in \{1, \dots, K\})$

$$y[m, k] = \|\mathbf{h}_t[k]\| u[m, k] + z[m, k], \quad t = \left\lfloor \frac{m}{M} \right\rfloor,$$

where $u[m, k] \sim \mathcal{CN}(0, P)$, and $(\forall t \in \mathbb{Z})$ $(\forall k \in \{1, \dots, K\})$,

$$\mathbf{h}_t[k] := \begin{bmatrix} \sum_{l=1}^{L/2} \beta_{l,t} e^{j(\theta_{l,t} + \phi_{l,k})} \\ \sum_{l=L/2+1}^L \beta_{l,t} e^{j(\theta_{l,t} + \phi_{l,k})} \end{bmatrix}.$$

The above scheme achieves the outage rate

$$R_{\text{out}} = \sup_{r \in \mathbb{R}} r \cdot \Pr \left(\frac{1}{K} \sum_{k=1}^K \log(1 + \|\mathbf{h}[k]\|^2 P) \geq r \right),$$

and the ergodic rate

$$R = \mathbb{E} \left[\frac{1}{K} \sum_{k=1}^K \log(1 + \|\mathbf{h}[k]\|^2 P) \right] = \mathbb{E}[\log(1 + \|\mathbf{h}\|^2 P)],$$

where $\mathbf{h} := [\sum_{l=1}^{L/2} \beta_l e^{j\theta_l} \quad \sum_{l=L/2+1}^L \beta_l e^{j\theta_l}]^T$ is the effective channel without phase diversity. Similar to non-coherent joint transmission, the use of phase diversity is motivated by the significant benefits it offers in terms of outage rate and simplification of rate adaptation / HARQ mechanisms for the ergodic regime. In particular, similar to non-coherent joint transmission, as K grows large, the instantaneous rate becomes essentially driven by the blockage process:

Proposition 7. Let $(\forall(i_1, i_2) \in \{0, \dots, L/2\}^2) \bar{R}(i_1, i_2) := \mathbb{E} \left[\log \left(1 + \left| \sum_{l=1}^{i_1} e^{j\theta_l} \right|^2 P + \left| \sum_{l=L/2+1}^{L/2+i_2} e^{j\theta_l} \right|^2 P \right) \right]$.

Then, $(\forall \epsilon > 0)$

$$\Pr \left(\left| \frac{1}{K} \sum_{k=1}^K \log(1 + \|\mathbf{h}[k]\|^2 P) - \bar{R}(\alpha_1, \alpha_2) \right| \geq \epsilon \right) \xrightarrow{K \rightarrow \infty} 0,$$

where $(\alpha_1, \alpha_2) := \left(\sum_{l=1}^{L/2} \beta_l, \sum_{l=L/2+1}^L \beta_l \right)$.

Proof. (Sketch) The proof is based on the weak law of large numbers and it is similar to the proof of Proposition ??.

Interestingly, Figure ?? and Figure ?? show that the above scheme is able to recover a significant fraction of both the outage and the ergodic capacity in most regimes of interest.

IV. Coarse time synchronization

We now assume that the network can jointly compensate the different physical propagation delays of the signals from different transmitters only up to some maximum timing offset $\tau_{\max} > 0$. As customary, we will use OFDM to provide robustness against unknown residual delays. In particular, we consider the time-domain channel model $(\forall m \in \mathbb{Z})$

$$y[m] = \sum_{l=1}^L (h_l * x_l)[m] + z[m],$$

where the impulse responses $h_l[m]$ for $l \in \{1, \dots, L\}$ model the intermittent block fading process and the intersymbol interference originating from the residual delays. Specifically, we let:

$$h_l[m] = h_{l,t} g(m - \tau_l), \quad h_{l,t} = \beta_{l,t} e^{j\theta_{l,t}}, \quad t = \left\lfloor \frac{m}{T} \right\rfloor,$$

where g is some continuous-time causal impulse response which models the convolution between the pulse shape and receiver filters, and $\tau_l \leq \tau_{\max}$ is an unknown and possibly non-integer residual delay for the l th transmitter. We assume for simplicity standard square pulses at the transmitter side and matched filtering at the receiver side, i.e., a triangular impulse response

$$g(x) = \begin{cases} 1 - |x|, & x \in (-1, 1) \\ 0, & \text{otherwise,} \end{cases}$$

as in basic OFDM implementations. Different pulses may give better performance, but we leave their analysis to future work.

Assuming an OFDM system with K subcarriers and a cyclic prefix of length $D \geq \lceil \tau_{\max} \rceil + 1$, such that an integer number $M = T/(K + D)$ of OFDM symbols are transmitted in each fading block, the channel model in the time-frequency domain is given by $(\forall m \in \mathbb{Z}) (\forall k \in \{0, \dots, K - 1\})$

$$Y[m, k] = \sum_{l=1}^L H_{l,t}[k] X_l[m, k] + Z[m, k], \quad t = \left\lfloor \frac{m}{M} \right\rfloor,$$

where $Z[m, k] \sim \mathcal{CN}(0, 1)$ is a sample of a white Gaussian noise process (in both time and frequency), and where $H_{l,t}[k]$ is the K -points discrete-time Fourier transform

(DFT) of $h_{l,t}[m]$. By splitting the delay τ_l into an integer part $d_l \in \mathbb{N}$ and a fractional part $\delta_l \in [0, 1)$ such that $\tau_l = d_l + \delta_l$, we obtain

$$H_{l,t}[k] = \beta_{l,t} e^{j\theta_{l,t}} e^{-j2\pi \frac{k}{K} d_l} G_l[k],$$

where $G_l[k] := (1 - \delta_l) + \delta_l e^{-j2\pi \frac{k}{K}}$ is the DFT of $g(m - \delta_l)$.

A. Capacity

To capture the impact of unknown and uncontrollable residual delays, we follow a worst-case approach similar to the information theoretical literature on asynchronous [?] or arbitrarily varying [?] channels, and define ergodic capacity as the maximum achievable ergodic rate for all possible delays $\boldsymbol{\tau} = (\tau_1, \dots, \tau_L) \in [0, \tau_{\max}]^L$. This implies that an upper bound on the ergodic capacity of the considered channel is readily given by the ergodic capacity under perfect time synchronization $C = \mathbb{E}[\log(1 + \alpha P)]$, studied in Proposition ??.

In addition, by applying for each subcarrier the signaling scheme achieving C , we obtain the following lower bound on the ergodic capacity:

$$R = \inf_{\boldsymbol{\tau} \in [0, \tau_{\max}]^L} \frac{1}{K + D} \sum_{k=0}^{K-1} \mathbb{E} \left[\log \left(1 + \sum_{l=1}^L |H_l[k]|^2 P \right) \right] \quad (8)$$

where $H_l[k] := \beta_{l,t} e^{j(\theta_{l,t} - 2\pi \frac{k}{K} d_l)} G_l[k]$ denotes a realization of $H_{l,t}[k]$. Inspecting the above equation shows that the integer parts $\mathbf{d} = (d_1, \dots, d_L)$ of the delays $\boldsymbol{\tau}$ contribute to capacity loss only through the cyclic prefix length D , i.e., the system is insensitive to their actual values. On the other hand, the fractional parts $\boldsymbol{\delta} = (\delta_1, \dots, \delta_L)$ contribute to capacity loss in a non-trivial manner through the induced frequency selectivity, i.e., through the fluctuations of $|G_l[k]|^2$ across the subcarriers.

It turns out that the ergodic rate R in (8) admits a closed form expression given by the intuitive case of completely off-grid sampling $(\forall l \in \{1, \dots, L\}) \delta_l = 0.5$.

Proposition 8. Consider the achievable ergodic rate (8). The following equality holds:

$$R = \frac{1}{K + D} \sum_{k=0}^{K-1} \mathbb{E} \left[\log \left(1 + \alpha \frac{P}{2} \left(1 + \cos \left(\frac{2\pi k}{K} \right) \right) \right) \right].$$

Furthermore,

$$\lim_{K \rightarrow \infty} R = \mathbb{E} \left[\log \left(1 + \alpha \frac{P}{4} + \frac{1}{2} (\sqrt{1 + \alpha P} - 1) \right) \right].$$

Proof. The proof is given in Appendix ??.

Following a similar worst-case approach, the outage capacity of the considered channel can be upper bounded by the outage capacity under perfect time synchronization

$$C_{\text{out}} = \max_{i \in \{1, \dots, L\}} \Pr(\alpha \geq i) \log(1 + iP),$$

and lower bounded by

$$R_{\text{out}} = \inf_{\boldsymbol{\tau} \in [0, \tau_{\max}]^L} \sup_{r \in \mathbb{R}} r \cdot \Pr \left(\frac{1}{K + D} \sum_{k=0}^{K-1} \log \left(1 + \sum_{l=1}^L |H_l[k]|^2 P \right) \geq r \right), \quad (9)$$

which can be characterized in closed form as stated next.